

E-Cadherin, NFATC3, and PLP2 Are Differentially Methylated in Multiple Cancers

Mary J Lotesto, Christopher J Wallace and Stacey L Raimondi 

Department of Biology, Elmhurst University, Elmhurst, IL, USA.

Epigenetics Insights
Volume 13: 1–14
© The Author(s) 2020
Article reuse guidelines:
sagepub.com/journals-permissions
DOI: 10.1177/2516865720964802



ABSTRACT: It is well documented that cancer cells have abnormal methylation patterns often caused by faulty methylating machinery. Specifically, *E-cadherin*, *NFATC3*, and *PLP2* are 3 genes known to be aberrantly methylated in cancer cells. These genes are well documented for their role in signaling pathways involved with cell proliferation, adhesion, migration, and other signs of tumor progression. Therefore, changes in gene expression of *CDH1*, *NFATC3*, and *PLP2* due to aberrant methylation can lead to profound changes in cellular function and tumor formation. In order to ensure that previous *in vitro* and *in vivo* methylation studies match what is observed in the clinic, we utilized a bioinformatics approach to complete an extensive analysis of methylation patterns of these 3 genes, analyzing over 5000 patient samples, across all cancers for which both normal and tumor tissues were available. Specifically, we analyzed overall and site-specific methylation patterns, at CpG islands and shores, of all 3 genes across 14 cancer types. Furthermore, we compared these methylation levels in normal and tumor samples of both matched and unmatched patient samples in order to determine any differences between groups. Finally, we examined whether an aberrant DNA methyltransferase, *DNMT3B7*, known to be expressed in cancer cells and to alter methylation patterns *in vitro* correlated with altered overall and site-specific methylation of *CDH1*, *NFATC3*, and *PLP2* in these patient samples. Our results indicate that methylation patterns of *CDH1* and *NFATC3* were unexpectedly varied across tumors, contrary to previous studies performed *in vitro*, while *PLP2* showed the expected hypomethylation pattern in tumor tissues. We also observed some correlation between *DNMT3B7* expression and methylation patterns of these genes, but patterns were inconsistent. Taken together, these results emphasize the necessity for *in vivo* and patient studies rather than a complete reliance on *in vitro* data and provide multiple areas of future research.

KEYWORDS: E-cadherin, NFATC3, PLP2, DNMT3B7, DNA methylation, cancer

RECEIVED: July 14, 2020. **ACCEPTED:** September 14, 2020.

TYPE: Original Research

FUNDING: The author(s) disclosed receipt of the following financial support for the research, authorship, and/or publication of this article: This work was supported by the Ellen Marks Foundation.

DECLARATION OF CONFLICTING INTERESTS: The author(s) declared no potential conflicts of interest with respect to the research, authorship, and/or publication of this article.

CORRESPONDING AUTHOR: Stacey L Raimondi, Department of Biology, Elmhurst University, 190 Prospect Ave., Box 133, Elmhurst, IL 60126, USA. Email: raimondis@elmhurst.edu

Introduction

Cancer is the second-leading cause of death globally and while treatments have improved and 5-year survival has increased for most cancers, there is still much that is unknown regarding the molecular mechanisms of tumor progression in patients.¹ Extensive studies have been performed *in vitro* and *in vivo* to answer these questions. However, there are limitations of *in vitro* work involving cancer cell lines, including the lack of interactions with other cell types which can affect drug delivery and metabolism.² Moreover, the likelihood of a phase I clinical trial leading to approval of a drug is, unfortunately, just 5.1%.³ Therefore, it is imperative that we ensure that our *in vitro* and *in vivo* findings are translatable. Fortunately, with the development of The Cancer Genome Atlas and Genomic Data Commons (GDC), it is becoming much easier to validate *in vitro* and *in vivo* findings in patient samples.

It is well documented that cancer cells display abnormal methylation patterns.^{4,5} Specifically, cancer cells tend to show an overall global hypomethylation leading to increased gene expression compared to normal cells. However, we also see examples of specific tumor suppressor genes which have been hypermethylated leading to a corresponding loss of gene expression. While most studies have focused on methylation of CpG dinucleotides within a larger CpG island near the promoter region, more recent studies have shown that methylation patterns at CpG shores, found approximately 2 kb from an

island, are more strongly associated with gene expression than CpG island methylation.⁶ Therefore, it is imperative that any methylation study that occurs in patient samples include an analysis of not just overall methylation, but also site-specific methylation in order to form a better understanding of methylation patterns in patients.

Three specific genes that have been shown to have altered methylation patterns in cancer cells are *Epithelial(E)-cadherin (CDH1)*, *nuclear factor of activated T cells 3 (NFATC3)*, and *proteolipid protein 2 (PLP2)*. E-cadherin is known for its role in maintaining cell-cell adhesions in normal epithelial cells. However, the literature is clear that hypermethylation of *CDH1*, and corresponding loss of RNA/protein expression, promotes an epithelial-to-mesenchymal transition leading to tumor progression in epithelial cancers.^{7–11} While the primary role of *NFATC3* is to function as a transcription factor responsible for promoting T-cell development and proliferation, as well as COX-2 dependent migration and angiogenesis within the immune system, studies have shown altered methylation patterns across a variety of cancers.^{12–16} Most studies have shown hypomethylation, and increased expression of *NFATC3*, corresponded with tumor progression using *in vitro* and animal models.^{12–15} However, one study utilizing ovarian cancer patient sample data from the GDC showed hypermethylation and decreased expression of *NFATC3* correlated with decreased survival.¹⁶ Therefore, while it was assumed that *NFATC3* is



hypomethylated in cancer, which would correspond with its known functional role, conflicting studies indicate a need for a more in-depth analysis in patient samples across cancer types. Finally, while not as well studied as *CDH1* and *NEATC3*, *PLP2* has an important role in tumor progression due to its ability to promote activation of the PI3K/Akt pathway. Because of this association, hypomethylation and increased expression of *PLP2* in cancer cells has been shown to promote cell proliferation, adhesion, and invasion.^{17–21} Taken together, these 3 genes represent examples of genes which are typically hypermethylated (*CDH1*) or hypomethylated (*PLP2*) in cancer cells, as well as an example of a gene with conflicting data (*NEATC3*). However, virtually all of these methylation studies have been performed *in vitro* or in animal models with very little patient data to verify the results. Therefore, it is imperative that we complete a more thorough analysis in patients to determine if these methylation patterns are maintained in patient samples. Furthermore, once we understand the methylation changes that are occurring in patients, we can better identify the role of faulty DNA methylating machinery in cancer in order to develop novel treatments.

DNA methyltransferases (DNMTs) are responsible for maintaining normal methylation patterns in cells.^{22–24} Specifically, DNMT1 is responsible for maintaining methylation patterns in adult cells while DNMT3A and DNMT3B are *de novo* methylases responsible for adding new methyl groups to CpG dinucleotides during early development. Aberrant versions of DNMT3B have been identified in both cancer cell lines and patient tumors, but not normal cells, and their functional role continues to be determined.^{25–30} One of these aberrant transcripts, *DNMT3B7*, has been shown to be expressed in multiple cancer types.^{25,30} Several studies have shown that expression of *DNMT3B7* promotes lymphomagenesis, breast cancer, and neuroblastoma progression through altered methylation patterns in these tumors both *in vitro* and *in vivo* using animal models.^{27–29} Specifically, our laboratory and others have shown that DNMT3B7 expression in cell lines led to increased methylation, and down-regulation of protein expression, of E-cadherin and decreased methylation of *NEATC3* and *PLP2*.^{25,30} While these findings are very intriguing, to date they have only been performed *in vitro* and there are no patient studies verifying the results. Therefore, it is imperative that we determine a clinical role for *DNMT3B7* and other aberrant DNMTs with regard to altered methylation patterns.

Taken together, it is clear that there is much that we still do not know about methylation patterns of genes and the role of aberrant DNMTs in patient samples. To that end, we have utilized a bioinformatics approach with patient data from the GDC to examine methylation patterns of *CDH1*, *NEATC3*, and *PLP2*. We analyzed over 5000 patient samples across 14 cancer types for which normal and tumor samples were available in order to examine changes in overall methylation as well as methylation at CpG islands and shores. This analysis was

completed in both matched and unmatched normal and tumor samples. We also assessed whether there was any correlation between aberrant *DNMT3B7* expression and methylation of these 3 genes. To our knowledge, this is the first analysis of this magnitude to occur and the results of this work provide important information regarding the future direction of methylation studies in patients.

Materials and Methods

Collection of data from Genomic Data Commons

RNAseqV2 and clinical data were obtained from the GDC Legacy data portal (<https://portal.gdc.cancer.gov/legacy-archive/search/f>) as previously described.^{28,30,31} Methylation data were collected from the GDC Data Portal (<https://portal.gdc.cancer.gov/repository>) and matched with corresponding *DNMT3B7* RNASeqV2 expression and clinical data using the unique “Case-UUID” number for each patient. All data were organized and processed using a custom C# script and Microsoft Excel (Redmond, Washington).

Statistical analysis

All statistical analysis was performed using SigmaStat software (Systat, Chicago, IL). Methylation values were obtained by either averaging all methylation sites for 1 gene together or separating by type of methylation site (Island, N_Shore, S_Shore) and then averaging all measures within a specific group. Primary tumor versus normal tissue methylation was compared using a *T*-test. A Mann-Whitney Rank Sum Test was used in situations where a normal distribution was not observed based on a Shapiro-Wilk Normality Test. Matched tissues were compared with a Paired *T*-Test or Signed Rank Test in the absence of a normal distribution. A Bonferroni correction was utilized for each cancer data set ($0.05/24=0.00208$) to avoid type I errors due to multiple comparisons. Correlation studies were performed using a Pearson Correlation Coefficient for normally distributed data or a Spearman Rank Order Correlation for data that did not have a normal distribution pattern. A Bonferroni correction was also utilized for each cancer data set ($0.05/12=0.00417$) to avoid type I errors.

Results

E-cadherin methylation patterns are varied across cancers

To begin our large-scale analysis of *CDH1* methylation, we utilized data from 14 cancer types and 5782 patient samples for which normal and tumor tissues were available on GDC. We compared methylation in all tumor samples to all normal tissues available as well as matched samples where we had normal and tumor tissue from the same patient. It was expected that we would observe increased methylation of *CDH1* in tumor tissues compared to normal samples based on the results of

previous studies.^{7–11} Of the 14 cancers tested, when we averaged all methylation sites across the entire gene for each patient, significant changes in *CDH1* methylation were only observed in 5 of them (BLCA, COAD, HNSC, LIHC, READ; Table 1). Interestingly, in 3 out of the 5 significant cancers, we observed the opposite methylation pattern from what was expected—hypomethylation of *CDH1* in tumor tissues. In cancers where matched normal and tumor tissues were available, we did not observe any significant difference in expression in the direction expected. All other cancers with matched samples either had no difference in methylation or hypomethylation of *CDH1* in tumor tissues compared to normal controls.

Because an average methylation value for a patient's specific gene does not provide site-specific information on methylation, and previous studies have shown that CpG shores are more likely to correspond to gene expression than any other methylation region,⁶ we undertook a more detailed analysis of methylation across all patient samples. Specifically, we calculated an average methylation value for every patient at the CpG island, N_Shore (the CpG shore located 5' to the island), and S_Shore (the CpG shore located 3' to the island; Table 2). Once again, only 5 cancers (BLCA, COAD, KIRC, KIRP, LIHC) out of 14 showed an altered methylation pattern in at least 1 methylation site, but they were not the same 5 cancers in which we observed significant results above. Interestingly, we still observed the same unexpected hypomethylation pattern seen in Table 1 in 3 cancers (BLCA, COAD, and LIHC) when we completed the in-depth analysis (Table 2). However, the cancers which showed the expected hypermethylation pattern changed between the 2 analyses.

NFATC3 is hypermethylated in most tumor tissues

To continue our analysis of methylation patterns across cancer patient samples, we measured average methylation of *NFATC3*, a gene for which the literature showed conflicting reports about methylation patterns.^{12–16} Because the majority of the literature showed that *NFATC3* was hypomethylated, and its known function implies that increased expression should correlate with tumor progression, we hypothesized that *NFATC3* would be hypomethylated in tumor tissues. Surprisingly, our analysis of average overall methylation shows that *NFATC3* is hypermethylated in 5 cancers (BRCA, COAD, KIRP, LUAD, READ) and hypomethylated in only 1 cancer (LIHC; Table 1), indicating that *NFATC3* is typically turned “off” in patients despite its role in promoting angiogenesis and chemoresistance. When we completed further analysis of methylation at the CpG island, N_Shore, and S_Shore, we found 3 additional cancers (HNSC, KIRC, LUSC; Table 3) that were also hypermethylated as well as some alterations in the methylation patterns observed in Table 1. For example, while we observed a significant difference in COAD overall methylation in unmatched samples (Table 1), we did not observe that same

change at any specific site in our more detailed analysis (Table 3). Interestingly, we did not observe hypomethylation at any site in any cancer when we completed our detailed analysis, even though LIHC had shown an overall hypomethylated pattern (Table 1).

PLP2 is hypomethylated in all cancers tested

Because of the unexpected findings observed in our analysis of *CDH1* and, especially, *NFATC3*, we examined an additional gene known to be hypomethylated in cancer—*PLP2*.^{17–21} As expected, overall *PLP2* methylation levels were reduced in all tumor types tested compared to normal tissues (Table 1). Furthermore, upon completion of our in-depth analysis of site-specific methylation, we observed the expected hypomethylation pattern across all cancers with significant results (Table 4).

DNMT3B7 expression is correlated to CDH1, NFATC3, or PLP2 methylation in some patient samples

Finally, to determine if *DNMT3B7* expression correlated with methylation of *CDH1*, *NFATC3*, and *PLP2*, we matched both overall methylation data, as well as methylation at individual islands and shores, to corresponding *DNMT3B7* expression. Pearson Correlation Coefficient or Spearman Rank Order Correlation analyses were conducted to determine if there was any correlation between *DNMT3B7* expression and overall, or site-specific, gene methylation in tumor tissue samples across cancers (Tables 5–8). Overall, correlation results were inconsistent across all cancers, and cancers which showed significant methylation changes between normal and tumor samples did not necessarily correlate with *DNMT3B7* expression. However, some interesting trends did arise. First of all, the only significant findings for *CDH1*, whether looking at overall or site-specific methylation, indicated a negative correlation which would imply that *CDH1* methylation decreases as *DNMT3B7* expression increases. Conversely, when *NFATC3* methylation correlated to *DNMT3B7* expression, it was always in a positive relationship. Finally, *PLP2*, the only gene that had shown a consistent methylation pattern above, showed an extremely inconsistent correlation pattern across cancers. In some cases it was negatively correlated with *DNMT3B7* (BRCA) and other times it was positively correlated in other cancers (BLCA, HNSC; Tables 5 and 8). In the case of site-specific methylation of *PLP2* in LUAD, there is a negative correlation with *DNMT3B7* at the CpG island and a positive correlation at the S_Shore (Table 8), indicating a need for future analysis.

Discussion

The results presented here clearly indicate that it is imperative that we utilize patient data as often as possible to verify results observed in *in vitro* and animal models. Fortunately, databases

Table 1. Statistical results of average overall methylation patterns for 3 genes across cancer types.

CANCER NAME	ABBREVIATION	SAMPLE SIZE	E-CADHERIN (CDH1)		NFATC3		PLP2	
			NORMAL TUMOR	MATCHED NORMAL VERSUS TUMOR	NORMAL TUMOR	MATCHED NORMAL VERSUS TUMOR	NORMAL TUMOR	MATCHED NORMAL VERSUS TUMOR
Bladder urothelial carcinoma	BLCA	427	(-) $P < .001$	(-) $P < .001$	$P = .141$	$P = .448$	(-) $P < .001$	(-) $P = .001$
Breast invasive carcinoma	BRCA	1062	$P = .448$	$P = .412$	(+) $P < .001$	(+) $P < .001$	(-) $P < .001$	(-) $P < .001$
Cervical squamous cell carcinoma and endocervical adenocarcinoma	CESC	307	$P = .832$	$P = .802$	$P = 0.211$	$P = .699$	$P = .420$	$P = .098$
Colon adenocarcinoma	COAD	332	$P = .651$	(-) $P < .001$	(+) $P < .001$	$P = .688$	$P = .021$	(-) $P = .001$
Esophageal carcinoma	ESCA	192	$P = .652$	$P = .322$	$P = .189$	$P = .008$	$P = .003$	$P = .528$
Head/neck squamous cell carcinoma	HNSC	542	(+) $P = .002$	$P = .388$	$P = .194$	$P = .848$	$P = .633$	$P = .331$
Kidney renal clear cell carcinoma	KIRC	342	$P = .189$	$P = .067$	$P = .071$	$P = .006$	$P = .076$	$P = .025$
Kidney renal papillary cell carcinoma	KIRP	293	$P = .048$	$P = .016$	(+) $P = .001$	(+) $P < .001$	$P = .058$	$P = .455$
Liver hepatocellular carcinoma	LHC	413	(-) $P < .001$	$P = .022$	(-) $P < .001$	$P = .123$	(-) $P < .001$	(-) $P < .001$
Lung adenocarcinoma	LUAD	533	$P = .693$	$P = .312$	(+) $P < .001$	$P = .956$	$P = .308$	$P = .009$
Lung squamous cell carcinoma	LUSC	509	$P = .400$	$P = .306$	$P = .222$	$P = .250$	$P = .040$	(-) $P = .001$
Rectum adenocarcinoma	READ	94	(+) $P < .001$	N/A	(+) $P < .001$	N/A	$P = .032$	N/A
Thyroid cancer	THCA	554	$P = .206$	$P = .320$	$P = .516$	$P = .199$	$P = .072$	$P = .004$
Uterine corpus endometrial carcinoma	UCEC	182	$P = .040$	N/A	$P = .050$	N/A	$P = .844$	N/A

Normal versus tumor includes all patient samples available while matched normal versus tumor only includes matched samples.

Statistically significant data ($P < .00208$ based on a Bonferroni correction of 0.05/24) shaded yellow.

(-) indicates that the gene is hypomethylated in tumor tissues compared to normal samples.

(+) indicates that the gene is hypermethylated in tumor tissues compared to normal samples.

Table 2. Statistical results for average methylation of *CDH1* at CpG island, N_Shore, and S_Shore.

CANCER NAME	ABBREVIATION	SAMPLE SIZE	ISLAND		N_SHORE		S_SHORE	
			NORMAL VERSUS TUMOR	MATCHED NORMAL VERSUS TUMOR	NORMAL VERSUS TUMOR	MATCHED NORMAL VERSUS TUMOR	NORMAL VERSUS TUMOR	MATCHED NORMAL VERSUS TUMOR
Bladder urothelial carcinoma	BLCA	427	(-) $P < .001$	(-) $P < .001$	(-) $P < .001$	(-) $P < .001$	(-) $P < .001$	(-) $P < .001$
Breast invasive carcinoma	BRCA	1062	$P = .155$	$P = .017$	$P = .927$	$P = .532$	$P = .006$	$P = .061$
Cervical squamous cell carcinoma and endocervical adenocarcinoma	CESC	307	$P = .372$	$P = .011$	$P = .246$	$P = .254$	$P = .842$	$P = .613$
Colon adenocarcinoma	COAD	332	(-) $P = .001$	(-) $P < .001$	(-) $P < .001$	(-) $P < .001$	$P = .874$	$P = .078$
Esophageal carcinoma	ESCA	192	$P = .773$	$P = .119$	$P = .320$	$P = .149$	$P = .907$	$P = .566$
Head/neck squamous cell carcinoma	HNSC	542	$P = .006$	$P = .349$	$P = .013$	$P = .368$	$P = .006$	$P = .073$
Kidney renal clear cell carcinoma	KIRC	342	(+) $P < .001$	(+) $P < .001$	(+) $P < .001$	(+) $P = .002$	(+) $P < .001$	(+) $P < .001$
Kidney renal papillary cell carcinoma	KIRP	293	$P = .059$	$P = .004$	(+) $P < .001$	(+) $P < .001$	$P = .209$	$P = .010$
Liver hepatocellular carcinoma	LIRC	413	$P = .020$	$P = .014$	$P = .266$	$P = .056$	(-) $P < .001$	(-) $P < .001$
Lung adenocarcinoma	LUAD	533	$P = .033$	$P = .806$	$P = .971$	$P = .695$	$P = .557$	$P = .786$
Lung squamous cell carcinoma	LUSC	509	$P = .237$	$P = .774$	$P = .671$	$P = .813$	$P = .200$	$P = .498$
Rectum adenocarcinoma	READ	94	$P = .238$	N/A	$P = .933$	N/A	$P = .461$	N/A
Thyroid cancer	THCA	554	$P = .157$	$P = .251$	$P = .171$	$P = .243$	$P = .594$	$P = .601$
Uterine corpus endometrial carcinoma	UCEC	182	$P = .280$	N/A	$P = .006$	N/A	$P = .184$	N/A

Normal versus tumor includes all patient samples available while matched normal versus tumor only includes matched samples.

Statistically significant data ($P < .00208$ based on a Bonferroni correction of 0.05/24) shaded yellow.

(-) indicates that *CDH1* is hypomethylated in tumor tissues compared to normal samples.

(+) indicates that *CDH1* is hypermethylated in tumor tissues compared to normal samples.

Table 3. Statistical results for average methylation of *NFATC3* at CpG island, N_Shore, and S_Shore.

CANCER NAME	ABBREVIATION	SAMPLE SIZE	ISLAND		N_SHORE		S_SHORE	
			NORMAL VERSUS TUMOR	MATCHED NORMAL VERSUS TUMOR	NORMAL VERSUS TUMOR	MATCHED NORMAL VERSUS TUMOR	NORMAL VERSUS TUMOR	MATCHED NORMAL VERSUS TUMOR
Bladder urothelial carcinoma	BLCA	427	$P = .457$	$P = .927$	$P = .760$	$P = .290$	$P = .883$	$P = .022$
Breast invasive carcinoma	BRCA	1062	(+) $P < .001$	(+) $P < .001$	(+) $P < .001$	(+) $P < .001$	$P = .779$	$P = .006$
Cervical squamous cell carcinoma and endocervical adenocarcinoma	CESC	307	$P = .904$	$P = .344$	$P = .251$	$P = .326$	$P = .013$	$P = .278$
Colon adenocarcinoma	COAD	332	$P = .078$	$P = .274$	$P = .784$	$P = .437$	$P = .692$	$P = .117$
Esophageal carcinoma	ESCA	192	$P = .258$	$P = 1.000$	$P = .015$	$P = .027$	$P = .641$	$P = .008$
Head/neck squamous cell carcinoma	HNSC	542	(+) $P < .001$	$P = .076$	$P = .011$	$P = .295$	$P = .773$	$P = .985$
Kidney renal clear cell carcinoma	KIRC	342	(+) $P < .001$	$P = .011$	(+) $P < .001$	(+) $P < .001$	(+) $P < .001$	$P = .020$
Kidney renal papillary cell carcinoma	KIRP	293	$P = .571$	$P = .173$	(+) $P < .001$	(+) $P < .001$	(+) $P < .001$	$P = .922$
Liver hepatocellular carcinoma	LIHC	413	(+) $P < .001$	(+) $P < .001$	$P = .079$	$P = .412$	(+) $P < .001$	(+) $P = .001$
Lung adenocarcinoma	LUAD	533	$P = .191$	$P = .546$	(+) $P < .001$	$P = .072$	$P = .162$	$P = .314$
Lung squamous cell carcinoma	LUSC	509	$P = .003$	$P = .641$	(+) $P < .001$	$P = .024$	$P = .059$	$P = .578$
Rectum adenocarcinoma	READ	94	$P = .113$	N/A	N/A	N/A	N/A	N/A
Thyroid cancer	THCA	554	$P = .523$	$P = .006$	$P = .017$	$P = .315$	$P = .004$	$P = .060$
Uterine corpus endometrial carcinoma	UCEC	182	$P = .755$	N/A	$P = .975$	N/A	$P = .206$	N/A

Normal versus tumor includes all patient samples available while matched normal versus tumor only includes matched samples. Statistically significant data ($P < .00208$ based on a Bonferroni correction of 0.05/24) shaded yellow. (+) indicates that *NFATC3* is hypermethylated in tumor tissues compared to normal samples.

Table 4. Statistical results for average methylation of *PLP2* at CpG island, N_Shore, and S_Shore.

CANCER NAME	ABBREVIATION	SAMPLE SIZE	/ISLAND		N_SHORE		S_SHORE	
			NORMAL VERSUS TUMOR	MATCHED NORMAL VERSUS TUMOR	NORMAL VERSUS TUMOR	MATCHED NORMAL VERSUS TUMOR	NORMAL VERSUS TUMOR	MATCHED NORMAL VERSUS TUMOR
Bladder urothelial carcinoma	BLCA	427	P = .011	P = .008	(-) P < .001	(-) P = .001	(-) P < .001	P = .101
Breast invasive carcinoma	BRCA	1062	P = .462	P = .198	(-) P < .001	(-) P < .001	(-) P < .001	(-) P < .001
Cervical squamous cell carcinoma and endocervical adenocarcinoma	CESC	307	P = .179	P = .080	P = .042	P = .250	P = .003	P = .055
Colon adenocarcinoma	COAD	332	P = .012	P = .298	P = .045	P = .012	P = .770	P = .518
Esophageal carcinoma	ESCA	192	P = .050	P = .820	P = .006	P = .649	(-) P < .001	P = .316
Head/neck squamous cell carcinoma	HNSC	542	P = .835	P = .812	P = .386	P = .783	P = .082	P = .008
Kidney renal clear cell carcinoma	KIRC	342	P = .242	P = .920	P = .138	P = .411	(-) P < .001	(-) P < .001
Kidney renal papillary cell carcinoma	KIRP	293	P = .230	P = .581	P = .600	P = 1.000	P = .010	P = .030
Liver hepatocellular carcinoma	LIHC	413	P = .059	P = .162	(-) P < .001	(-) P < .001	(-) P < .001	(-) P < .001
Lung adenocarcinoma	LUAD	533	P = .657	P = .522	P = .086	(-) P < .001	P = .864	P = .031
Lung squamous cell carcinoma	LUSC	509	P = .027	P = .710	P = .024	(-) P = .002	P = .008	(-) P = .002
Rectum adenocarcinoma	READ	94	P = .005	N/A	P = .037	N/A	N/A	N/A
Thyroid cancer	THCA	554	P = .285	P = .082	P = .354	P = .390	P = .106	P = .032
Uterine corpus endometrial carcinoma	UCEC	182	P = .119	N/A	P = .117	N/A	P = .025	N/A

Normal versus tumor includes all patient samples available while matched normal versus tumor only includes matched samples. Statistically significant data ($P < .00208$ based on a Bonferroni correction of 0.05/24) shaded yellow. (-) indicates that *PLP2* is hypomethylated in tumor tissues compared to normal samples.

Table 5. Correlation results for overall methylation of all 3 genes versus DNMT3B7 across cancer types.

CANCER NAME	ABBREVIATION	SAMPLE SIZE	E-CADHERIN (CDH1)		NFATC3		PLP2	
			R ^a	P	R ^b	P	R ^b	P
Bladder urothelial carcinoma	BLCA	427	-0.0693 (rP)	.161	+0.0371	.454	+0.0794	0.108
Breast invasive carcinoma	BRCA	1062	-0.0421	.193	+0.0510	.114	-0.122	.000150
Cervical squamous cell carcinoma and endocervical adenocarcinoma	CESC	307	-0.161	.00480	-0.0872	.129	-0.0747	.194
Colon adenocarcinoma	COAD	332	-0.0504	.385	-0.0346	.551	-0.0256	.659
Esophageal carcinoma	ESCA	192	-0.0582 (rP)	.425	+0.0878	.237	-0.0249	.738
Head/neck squamous cell carcinoma	HNSC	542	-0.0241	.583	+0.0691	.115	+0.137	.00173
Kidney renal clear cell carcinoma	KIRC	342	-0.0576	.0933	+0.0324	.564	+0.0357	.525
Kidney renal papillary cell carcinoma	KIRP	293	-0.0685	.231	+0.104	.0866	+0.0976	.109
Liver hepatocellular carcinoma	LIHC	413	-0.159	.00217	-0.0240	.645	+0.0281	.590
Lung adenocarcinoma	LUAD	533	+0.0281	.525	+0.224	.000000308	-0.101	.0226
Lung squamous cell carcinoma	LUSC	509	-0.101	.0237	+0.116	.00921	-0.0911	.0416
Rectum adenocarcinoma	READ	94	+0.0444	.679	-0.0875	.414	-0.0416	.698
Thyroid cancer	THCA	554	-0.113	.0105	+0.102	.0222	+0.0242	.588
Uterine corpus endometrial carcinoma	UCEC	182	+0.0233	.757	-0.0284	.707	-0.0619	.411

Statistically significant data ($P < .00417$ based on a Bonferroni correction of 0.05/12) shaded yellow.

(rP), Pearson correlation coefficient.

^aR measured by Spearman rank order correlation (rS) unless otherwise notated.

(-) indicates negative correlation coefficient.

(+) indicates positive correlation coefficient.

Table 6. Correlation results for *CDH1* at CpG islands, N_Shore, and S_Shore compared to *DNMT3B7* expression.

CANCER NAME	ABBREVIATION	SAMPLE SIZE	/SLAND		N_SHORE		S_SHORE	
			R ^a	P	R ^a	P	R ^a	P
Bladder urothelial carcinoma	BLCA	427	-0.124	.0120	-0.144	.00351	-0.167	.000687
Breast invasive carcinoma	BRCA	1062	-0.00194	.952	-0.00521	.872	-0.00817	.800
Cervical squamous cell carcinoma and endocervical adenocarcinoma	CESC	307	-0.167	.00358	-0.158	.00579	-0.162	.00470
Colon adenocarcinoma	COAD	332	-0.177	.00214	-0.151	.00912	-0.150	.00925
Esophageal carcinoma	ESCA	192	-0.196	.00776	-0.141	.0574	-0.153	.0389
Head/neck squamous cell carcinoma	HNSC	542	-0.0758	.0844	-0.0594	.176	-0.0453	.302
Kidney renal clear cell carcinoma	KIRC	342	+0.0502	.372	+0.0518	.357	+0.0163	.772
Kidney renal papillary cell carcinoma	KIRP	293	-0.138	.0236	+0.0685	.261	-0.163	.00729
Liver hepatocellular carcinoma	LIHC	413	-0.0636	.222	-0.144	.00540	-0.0538	.301
Lung adenocarcinoma	LUAD	533	-0.0316	.475	-0.0672	.129	-0.0500 (rP)	.259
Lung squamous cell carcinoma	LUSC	509	-0.282	1.45E-010	-0.325	1.144E-013	-0.293	2.742E-011
Rectum adenocarcinoma	READ	94	+0.0200	.852	-0.00746	.945	+0.0386 (rP)	.720
Thyroid cancer	THCA	554	-0.115	.00987	-0.126	.00459	-0.167	.000167
Uterine corpus endometrial carcinoma	UCEC	182	+0.0111	.883	-0.148	.0482	-0.0398	.597

Statistically significant data ($P < .00417$ based on a Bonferroni correction of 0.05/12) shaded yellow.

(rP), Pearson correlation coefficient.

^aR measured by Spearman rank order correlation (rS) unless otherwise notated.

(-) indicates negative correlation coefficient.

(+) indicates positive correlation coefficient.

Table 7. Correlation results for NFATC3 at CpG islands, N_Shore, and S_Shore compared to DNMT3B7 expression.

CANCER NAME	ABBREVIATION	SAMPLE SIZE	ISLAND		N_SHORE		S_SHORE	
			R ^a	P	R ^a	P	R ^a	P
Bladder urothelial carcinoma	BLCA	427	+0.0445	.369	-0.0901	.0685	-0.0116	.815
Breast invasive carcinoma	BRCA	1062	+0.112	.000502	+0.0328	.403	-0.0424	.280
Cervical squamous cell carcinoma and endocervical adenocarcinoma	CESC	307	-0.0380	.509	-0.0726	.207	+0.0196	.733
Colon adenocarcinoma	COAD	332	-0.0563	.332	-0.0306	.604	-0.0635	.282
Esophageal carcinoma	ESCA	192	+0.151	.0410	+0.148	.0451	+0.0865	.244
Head/neck squamous cell carcinoma	HNSC	542	+0.0500	.255	+0.0712	.105	+0.0421	.338
Kidney renal clear cell carcinoma	KIRC	342	-0.0306	.587	+0.00851	.880	+0.0699	.214
Kidney renal papillary cell carcinoma	KIRP	293	-0.0114	.852	+0.201 (rP)	.000875	-0.0608	.318
Liver hepatocellular carcinoma	LIHC	413	+0.0461	.376	-0.0264	.611	+0.0499	.337
Lung adenocarcinoma	LJAD	533	+0.0312	.481	+0.0879	.0633	+0.182	.000108
Lung squamous cell carcinoma	LUSC	509	+0.0401	.371	+0.0895	.0857	+0.120	.0214
Rectum adenocarcinoma	READ	94	-0.0990	.355	-0.0296 (rP)	.785	+0.121	.261
Thyroid cancer	THCA	554	+0.152	.000628	+0.133	.00281	-0.00830	.853
Uterine corpus endometrial carcinoma	UCEC	182	-0.0987	.190	-0.165	.0535	+0.0229	.789

Statistically significant data ($P < .00417$ based on a Bonferroni correction of 0.05/12) shaded yellow.

(rP), Pearson correlation coefficient.

^aR measured by Spearman rank order correlation (rS) unless otherwise notated.

(-) indicates negative correlation coefficient.

(+) indicates positive correlation coefficient.

Table 8. Correlation results for PLP2 at CpG islands, N_Shore, and S_Shore compared to DNMT3B7 expression.

CANCER NAME	ABBREVIATION	SAMPLE SIZE	ISLAND		N_SHORE		S_SHORE	
			R ^a	P	R ^a	P	R ^a	P
Bladder urothelial carcinoma	BLCA	427	-0.0520	.293	+0.0279	.572	+0.234	.00000178
Breast invasive carcinoma	BRCA	1062	-0.0892	.00569	-0.155	.00000151	+0.129 (rP)	.000993
Cervical squamous cell carcinoma and endocervical adenocarcinoma	CESC	307	-0.0730	.204	-0.0596	.300	-0.0208	.718
Colon adenocarcinoma	COAD	332	-0.152	.00831	-0.0361	.534	+0.157	.00765
Esophageal carcinoma	ESCA	192	-0.0686	.355	-0.0475	.523	+0.0301	.686
Head/neck squamous cell carcinoma	HNSC	542	+0.126	.00389	+0.138	.00158	+0.117	.00777
Kidney renal clear cell carcinoma	KIRC	342	+0.0253	.654	+0.0747	.184	+0.0245	.663
Kidney renal papillary cell carcinoma	KIRP	293	+0.112	.0659	+0.141	.0200	+0.0179	.769
Liver hepatocellular carcinoma	LIHC	413	+0.0475	.361	-0.00278	.957	+0.0375	.471
Lung adenocarcinoma	LUAD	533	-0.147	.000878	-0.0986	.0257	+0.165	.000476
Lung squamous cell carcinoma	LUSC	509	-0.0358	.424	-0.106	.0172	-0.113	.0302
Rectum adenocarcinoma	READ	94	-0.140	.191	-0.0486	.651	+0.121	.262
Thyroid cancer	THCA	554	-0.00358	.936	+0.0308	.490	+0.125	.00483
Uterine corpus endometrial carcinoma	UCEC	182	-0.0249	.742	-0.119	.112	+0.00615	.943

Statistically significant data ($P < .00417$ based on a Bonferroni correction of 0.05/12) shaded yellow.

(rP), Pearson correlation coefficient.

^aR measured by Spearman rank order correlation (rS) unless otherwise notated.

(-) indicates negative correlation coefficient.

(+) indicates positive correlation coefficient.

like the GDC are making that work far easier to do than it was in the past. While the literature have been clear that *CDH1* is hypermethylated and *NFATC3* and *PLP2* are hypomethylated in other cancer models, those results were not consistently seen when we examined patient data at this large scale. While scientists are aware of the biological constraints that occur when using *in vitro* models, the unexpected results shown here indicate that some facts that we have held to be true may not be as universal as once expected. If we are going to successfully develop novel therapeutics to improve patient outcomes, we must understand what is happening in patients, rather than rely primarily on *in vitro* work, to direct our long-term drug development.

Perhaps the most surprising results we obtained were from the analysis of methylation status of *CDH1* across cancers. The hypermethylation of *CDH1* leading to decreased E-cadherin protein levels to promote epithelial-to-mesenchymal transition, tumor progression, and metastasis is well documented.^{7–11} There are no conflicting results in the literature pertaining to methylation status of *CDH1* in epithelial tumors, yet our results indicate that in half of the tumors for which we have significant data, *CDH1* is hypomethylated, not hypermethylated (Tables 1 and 2). This cannot be explained by differences in tumor type because these results were observed in epithelial, not mesenchymal, tumors. One possible explanation is that our previous work has shown that a preponderance of patient samples available on GDC are from patients with early stage tumors rather than later stage tumors.³⁰ Loss of E-cadherin and epithelial-to-mesenchymal transition is associated with a more aggressive, late-stage, disease so it is possible that these altered results are due to an uneven balance of samples across stages rather than a new paradigm in E-cadherin research. Nevertheless, these data demonstrate the importance of continuing to collect samples from cancer patients at all stages of their disease in order to obtain the best data sets for future studies.

In the case of *NFATC3*, while some studies indicated that it was hypomethylated with increased expression in cancer cells leading to proliferation, migration, angiogenesis, and chemoresistance, other studies show poor survival correlated with decreased expression and hypermethylation.^{12–16} It should be noted that many of the studies showing hypomethylation of *NFATC3* were completed using *in vitro* models. However, orthotopic mouse models have also shown that silencing of *NFATC3* led to tumor regression.¹⁵ Furthermore, another study indicated that increased expression of *NFATC3* correlated with chemoresistance in patients.¹² Taken together, these studies would indicate that hypomethylation of *NFATC3* leads to tumor progression. The only study, prior to this, that showed hypermethylation of *NFATC3* corresponded to decreased survival also utilized data from GDC, matching the results we obtained here (Tables 1 and 3).¹⁶ Taken together, these findings lead us to question which data are accurate. It is possible that, similar to the aforementioned unexpected E-cadherin results, the types of patient samples collected for the GDC are biasing our analysis in one direction. For example, if the GDC

patient samples are primarily those in early stages of disease, we would not expect to see markers of chemoresistance and angiogenesis, such as the hypomethylation of *NFATC3*, in these samples. While multiple laboratories have now shown similar results when utilizing the GDC data for analysis, these results are not necessarily matching the rest of the literature. Therefore, it is imperative that we ensure a well-represented sample is available in all studies before drawing any conclusions on the role of *NFATC3* in promoting tumor progression.

PLP2 was the only gene analyzed in this study for which both the *in vitro* and patient sample data completely corresponded (Tables 1 and 4).^{17–21} No matter the cancer type involved, *PLP2* was clearly hypomethylated. Because of its known role in promoting tumor progression through activation of the PI3K/Akt pathway, *PLP2* is an exciting target for future studies. While *PLP2* is not nearly as well-known or well-studied as *CDH1* or *NFATC3*, the results shown here that match previous *in vitro* work indicate its potential importance in future clinical studies.

Finally, while DNMT3B7 has been shown to be highly expressed in virtually all cancer types, and its expression promotes aberrant methylation of various genes *in vitro* and in animal models, we observed only a few correlations between DNMT3B7 expression and the methylation status of *CDH1*, *NFATC3*, or *PLP2* in patient tumor samples across cancers (Tables 5–8).^{25,27–30} Specifically, we observed a negative correlation with *CDH1* in 6 cancers (Tables 5 and 6), a positive correlation with *NFATC3* in 4 cancers (Tables 5 and 7), and a mix of positive and negative correlations with *PLP2* across 4 cancers (Tables 5 and 8). In the case of *CDH1*, these results are contrary to what we have previously observed *in vitro* showing DNMT3B7 expression leading to hypermethylation of *CDH1* in breast cancer cell lines, but would match with the findings above (Tables 1 and 2) showing a hypomethylation pattern in cancers known to have significantly increased DNMT3B7 levels.³⁰ Furthermore, the fact that significant correlations were observed at every methylation site in LUSC indicates that future research should examine this relationship more closely (Table 6). Some of the first studies identifying aberrant DNMTs were performed in lung cancers,²⁶ so it is perhaps not surprising to see significant correlations in this particular cancer type.

While the *NFATC3* findings showing positive correlation data was unexpected, it matches the data seen in Tables 1 and 3. Unlike with *CDH1* we did not observe any consistent correlations across any one cancer type, but this may be because previous *NFATC3* studies have focused on leukemias which were not part of this analysis. Similar to *CDH1*, if and when the data are available, this may be another area of future research. Finally, for *PLP2*, the inconsistent correlation findings are confounding, especially in the case of LUAD in which there was a negative correlation in the CpG island and a positive correlation in the S_Shore (Table 8). We do not have an explanation for these findings other than to say that it is clear that additional research

is needed to understand what is happening not only across cancers, but also in LUAD specifically.

While these correlation results were surprising, there are some confounding factors that may also be affecting our findings. First, the data available on GDC only allow an analysis of *DNMT3B7* gene expression, not protein expression. While it is known that gene expression does not always correlate with protein expression in cells,³² previous *DNMT3B7* studies have shown that expression at the DNA/RNA level has corresponded to protein expression in cell lines and animal models.^{25,27–30} However, it should be noted that previous studies have also shown that DNMT1 is post-translationally regulated so that RNA expression does not match protein expression.³³ While these results imply a similar process could occur in *DNMT3B7*, the site of post-translational regulation in the N-terminus of DNMT1 does not exist in either DNMT3A or DNMT3B. Indeed, the structure of the N-terminal region of DNMT1 is completely different from that of either DNMT3 gene. Therefore, we would not expect DNMT3B to undergo the same type of post-translational modification based on the known structure. Unfortunately, because *DNMT3B7* is an aberrantly spliced gene and truncated protein, its protein expression is not measured by the typical methods used to supply information to databases like GDC. Therefore, while we can determine that patients express *DNMT3B7*, we do not know how that correlates to protein levels in these patients. While the results from *in vitro* and animal models are promising, our analysis of methylation patterns indicates that *in vitro* studies do not always match with patient data. Therefore, we cannot draw any definitive conclusions about the lack of correlation at this time. Furthermore, Ostler and colleagues have shown that when *DNMT3B7* is active in cells, it is localized in the nucleus even though it lacks its strongest nuclear localization sequence.²⁵ It is unknown how *DNMT3B7* is able to enter the nucleus, but one hypothesis is that a normal DNMT carries it into the nucleus and *DNMT3B7* may work either alone or in collaboration with that normal DNMT to regulate methylation patterns. To date, that hypothesis has not been supported by any experimental evidence, but the possibility is still there. Unfortunately, due to the nature of bioinformatics we cannot test either the localization or binding to other proteins with the data available, so there is still much we do not understand about *DNMT3B7* in patient tissues.

Taken together, this study emphasizes the necessity of including patient samples with *in vitro* work in order to verify results observed in the closed system of cell lines. Fortunately, with the growing amount of data publicly available on various bioinformatics databases, correlating *in vitro* results to clinical samples is becoming easier and more cost effective than in previous decades. It is hoped that an increased reliance on patient data in the future will save researchers valuable time, money, and effort in preclinical drug development studies that will lead to better diagnosis, treatment, and survival of patients.


Acknowledgements

The authors wish to thank Mark Raimondi for writing all of the code needed to produce our data sets.

Authors' Contributions

MJL, CJW, and SLR conducted the statistical analyses, interpreted the data, and drafted the manuscript. SLR was responsible for conceptualization, methodology, data collection, and final proofreading of the manuscript.

ORCID iD

Stacey L Raimondi  <https://orcid.org/0000-0001-7667-6814>

REFERENCES

1. Cancer Fact Sheet [Internet]. World Health Organization. <https://www.who.int/news-room/fact-sheets/detail/cancer>. Accessed February 13, 2020.
2. Weinstein J. Cell lines battle cancer. *Nature*. 2012;483:544–545.
3. *Clinical Development Success Rates 2006–2015* [Internet]. *BIO industry analysis*. June 2016. <https://www.bio.org/sites/default/files/legacy/bioorg/docs/Clinical%20Development%20Success%20Rates%202006-2015%20-%20BIO,%20Biomedtracker,%20Amplion%202016.pdf>. Accessed February 13, 2020.
4. Robertson KD. DNA methylation and human disease. *Nat Rev Genet*. 2005;6:597–610.
5. Esteller M. Epigenetic gene silencing in cancer: the DNA hypermethylation. *Hum Mol Genet*. 2007;16:R50–59.
6. Irizarry RA, Ladd-Acosta C, Wen B, et al. The human colon cancer methylome shows similar hypo- and hypermethylation at conserved tissue-specific CpG island shores. *Nat Gen*. 2009;41:178–186. doi:10.1038/ng.298.
7. Graff JR, Gabrielson E, Fujii H, Baylin SB, Herman JG. Methylation patterns of the E-cadherin 5' CpG island are unstable and reflect the dynamic, heterogeneous loss of E-cadherin expression during metastatic progression. *J Biol Chem*. 2000;275:2727–2732.
8. Kudo Y, Kitajima S, Ogawa I, et al. Invasion and metastasis of oral cancer cells require methylation of E-cadherin and/or degradation of membranous beta-catenin. *Clin Cancer Res*. 2004;10:5455–5463.
9. Azarschab P, Stembalska A, Loncar MB, Pfister M, Sasiadek MM, Blin N. Epigenetic control of E-cadherin (CDH1) by CpG methylation in metastasising laryngeal cancer. *Oncol Rep*. 2003;10:501–503.
10. Holubekova V, Mendelova A, Grendar M, et al. Methylation pattern of *CDH1* promoter and its association with *CDH1* gene expression in cytological cervical specimens. *Oncol Lett*. 2016;12:2613–2621.
11. Hosoda K, Yashima K, Tamoto A, et al. Expression of methylation-modulated tumor-related genes in endoscopically resected early esophageal squamous neoplasia. *Oncol Lett*. 2017;14:737–742.
12. Ma X, Chen Z, Hua D, et al. Essential role for TrpC5-containing extracellular vesicles in breast cancer with chemotherapeutic resistance. *Proc Natl Acad Sci USA*. 2014;111:6389–6394.
13. Urso K, Alfranca A, Martinez-Martinez S, et al. NFATc3 regulates the transcription of genes involved in T-cell activation and angiogenesis. *Blood*. 2011;118:795–803.
14. Lee SH, Kieu C, Martin CE, et al. NFATc3 plays an oncogenic role in oral/oropharyngeal squamous cell carcinomas by promoting cancer stemness via expression of OCT4. *Oncotarget*. 2019;10(23):2306–2319.
15. Urso K, Fernandez A, Velasco P, et al. NFATc3 controls tumour growth by regulating proliferation and migration of human astrogloma cells. *Sci Rep*. 2019;9:9361. doi:10.1038/s41598-019-45731-w.
16. Dai W, Teodoridis JM, Zeller C, et al. Systematic CpG islands methylation profiling of genes in the Wnt pathway in epithelial ovarian cancer identifies biomarkers of progression-free survival. *Clin Cancer Res*. 2011;17:4052–4062.
17. Longo A, Librizzi M, Luparello C. Effect of transfection with PLP2 antisense oligonucleotides on gene expression of cadmium-treated MDA-MB231 breast cancer cells. *Anal Bioanal Chem*. 2013;405:1893–1901.
18. Zimmerman JW, Pennison MJ, Brezovich I, et al. Cancer cell proliferation is inhibited by specific modulation frequencies. *Br J Cancer*. 2012;106:307–313.
19. Lee SM, Shin H, Jang SW, et al. PLP2/A4 interacts with CCR1 and stimulates migration of CCR1-expressing HOS cells. *Biochem Biophys Res Commun*. 2004;324:768–772.
20. Sonoda Y, Warita M, Suzuki T, et al. Proteolipid protein 2 is associated with melanoma metastasis. *Oncol Rep*. 2010;23:371–376.
21. Ozawa H, Sonoda Y, Suzuki T, Yoshida-Hoshina N, Funakoshi-Tago M, Kasahara T. Knockdown of proteolipid protein 2 or focal adhesion kinase with an

- artificial microRNA reduces growth and metastasis of B16BL6 melanoma cells. *Oncol Lett.* 2012;3:19-24.
22. Bestor TH. The DNA methyltransferases of mammals. *Hum Mol Genet.* 2000;9:2395-2402.
 23. Okano M, Bell DW, Haber DA, Li E. DNA methyltransferases Dnmt3a and Dnmt3b are essential for de novo methylation and mammalian development. *Cell.* 1999;99:247-257.
 24. Reik W, Dean W, Walter J. Epigenetic reprogramming in mammalian development. *Science.* 2001;293:1089-1093.
 25. Ostler KR, Davis EM, Payne SL, et al. Cancer cells express aberrant DNMT3B transcripts encoding truncated proteins. *Oncogene.* 2007;26:5553-5563.
 26. Wang L, Wang J, Sun S, et al. A novel DNMT3B subfamily, DeltaDNMT3B, is the predominant form of DNMT3B in non-small cell lung cancer. *Int J Oncol.* 2006;29:201-207.
 27. Shah MY, Vasanthakumar A, Barnes NY, et al. DNMT3B7, a truncated DNMT3B isoform expressed in human tumors, disrupts embryonic development and accelerates lymphomagenesis. *Cancer Res.* 2010;70:5840-5850.
 28. Brambert PR, Kelsch DJ, Hameed R, et al. DNMT3B7 expression promotes tumor progression to a more aggressive phenotype in breast cancer cells. *PLoS ONE.* 2015;10:e0117310. doi:10.1371/journal.pone.0117310.
 29. Ostler KR, Yang Q, Looney TJ, et al. Truncated DNMT3B isoform DNMT3B7 suppresses growth, induces differentiation, and alters DNA methylation in human neuroblastoma. *Cancer Res.* 2012;72:4714-4723.
 30. Siddiqui S, White MW, Schroeder AM, DeLuca NV, Leszczynski AL, Raimondi SL. Aberrant DNMT3B7 expression correlates to tissue type, stage, and survival across cancers. *PLoS ONE.* 2018;13:e0201522. doi:10.1371/journal.pone.0201522.
 31. Grossman RL, Heath AP, Ferretti V, et al. Toward a shared vision for cancer genomic data. *New Eng J Med.* 2016;375:1109-1112.
 32. Liu Y, Beyer A, Aebersold R. On the dependency of cellular protein levels and mRNA abundance. *Cell.* 2016;165:535-550.
 33. Estève PO, Chin HG, Benner J, et al. Regulation of DNMT1 stability through SET7-mediated lysine methylation in mammalian cells. *Proc Natl Acad Sci USA.* 2009;106:5076-5081. doi:10.1073/pnas.0810362106.